J. Chem. Sci. Vol. 127, No. 10, October 2015, pp. 1687–1699.
DOI 10.1007/s12039-015-0939-2

Modelling Gas Adsorption in Porous Solids: Roles of Surface Chemistry and Pore Architecture

SATYANARAYANA BONAKALA and SUNDARAM BALASUBRAMANIAN*
Chemistry and Physics of Materials Unit, Jawaharlal Nehru Centre for Advanced Scientific Research, Bangalore 560 064, India
e-mail: bala@jncasr.ac.in

MS received 18 May 2015; revised 29 June 2015; accepted 16 July 2015

Abstract. Modelling the adsorption of small molecule gases such as N_2, CH_4 and CO_2 in porous solids can provide valuable insights for the development of next generation materials. Employing a grand canonical Monte Carlo simulation code developed in our group, the adsorption isotherms of CH_4 and CO_2 in many metal organic frameworks have been calculated and compared with experimental results. The isotherms computed within a force field approach are able to well reproduce the experimental data. Key functional groups in the solids which interact with gas molecules and the nature of their interactions have been identified. The most favorable interaction sites for CH_4 and CO_2 in the framework solids are located in the linkers which are directed towards the pores. The structure of a perfluorinated conjugated microporous polymer has been modelled and it is predicted to take up 10% more CO_2 than its hydrogenated counterpart. In addition, the vibrational, orientational and diffusive properties of CO_2 adsorbed in the solids have been examined using molecular dynamics simulations. Intermolecular modes of such adsorbed species exhibit a blue shift with increasing gas pressure.

Keywords. Monte Carlo simulations; metal organic frameworks; Grand Canonical Monte Carlo; adsorption isotherm.

1. Introduction

Adsorption of gases in porous solids has received a lot of attention over the past several decades not only from a fundamental point of view, but also towards many applications including the development of efficient and environmentally benign energy materials.[1] Materials for storage of gases such as H_2,[2–4] O_2,[5] and CH_4[6–8] are important in energy applications and that for CO_2[9,10] in the environmental domain. Both volumetric and gravimetric[11–14] uptake by a substance are important quantities to judge its applicability for gas storage. Apart from pore size, pore volume and surface area of the adsorbent,[15,16] gas uptake is strongly influenced by its chemical characteristics,[17] the accessibility of its pores to the gas molecule and temperature.[18–21]

Modelling of adsorption isotherms is essential to develop a microscopic understanding of gas adsorption and gas-solid interactions. Various computational techniques have been adopted to model gas adsorption and separation of gases using porous solids. For a comprehensive review, see Ref.[22] One of the important modelling methods for studying adsorption is the grand canonical Monte Carlo (GCMC) simulation, carried out in the constant μVT ensemble. The average number of molecules adsorbed as a function of pressure, i.e., the adsorption isotherm can be obtained from a GCMC simulation.[23–36] While several open source Monte Carlo simulation programs are available such as the MCCCS Towhee,[37] Etomica,[38] BOSS,[39] DL_MONTE[23] and MUSIC.[40] Results reported here are obtained through a code developed in-house called MCIN.

In the present work, we focus on studying the adsorption of CO_2 and CH_4 in many metal organic framework (MOF) solids. The MOFs considered here are well characterized experimentally, both in terms of crystal structure and through adsorption isotherms for either CH_4 and/or CO_2. They possess different organic linker groups with varied functionalities. Thus, one can obtain a microscopic rationalization of gas uptake in these systems, an aspect which has not yet been studied using simulations. In addition, we have also examined the adsorption of CO_2 in a yet to be synthesized, perfluorinated amorphous polymer. One of the key results that have emerged from our investigations is that for a proper reproduction of experimental isotherms, consideration of electrostatic interactions between CO_2 molecules is necessary while that of the same between the gas and the framework appears not to be as relevant.

*For correspondence

We have also been able to predict an increased uptake of CO_2 by an amorphous polymer upon its perfluorination. The manuscript is divided as follows. Following this Introduction, we present details of the simulations of gas adsorption in several MOFs and of modelling the amorphous polymer. Subsequently, results from the simulations are presented, followed by conclusions drawn.

2. Computational details

2.1 *GCMC Simulations using MCIN*

Details of implementation of the GCMC code, its capabilities and validation are provided in Supplementary Information. Here, we provide the setup, potentials and other run details for each of the system studied. The adsorbents chosen have been well studied experimentally in terms of structure and gas (CH_4 or CO_2) adsorption characteristics.

2.1a *CH_4 adsorption*: We studied the adsorption isotherms of CH_4 in FMOF-1, $(Ag_2[Ag_4Tz_6])_n$, where Tz = 3,5-bis (trifluoromethyl) [1,2,4- triazolate][41] and $[Zn_2(L)]_\infty$, L = 4, 4′ -bipyridine-2,6,2′[42] MOF. FMOF-1 is quite hydrophobic due to perfluorinated ligands and exhibits a high uptake of hydrocarbons over water vapour.[43] $[Zn_2(L)]_\infty$ is demonstrated to show tremendous thermal stability and reversible uptake of several organics.[42] A cutoff distance of 12.8 Å was used for LJ interactions. Cavity biased GCMC simulations were carried out (see Supporting Information for details). Framework atoms were treated using the universal force field (UFF)[44] and CH_4 molecule was considered as a single LJ interaction site with parameters taken from the TraPPE force field.[45] Thus, rotational moves for the adsorbate were not necessary. At each state point, the GCMC simulation consisted of 1×10^7 steps devoted towards equilibration followed by 2×10^8 steps to sample the desired thermodynamic properties. Values of 0.8 σ and 0.5 σ were used as cavity radii at low and higher pressures respectively. The details of the GCMC simulations are tabulated in table 1.

2.2 *CO_2 adsorption*

2.2a *Zn(NDC)(DMBI) MOF*: We performed GCMC simulations using MCIN to study the adsorption isotherms of CO_2 in a microporous framework, Zn(NDC)(DPMBI) (where NDC=2,7-naphthalene dicarboxylate and DPMBI=N,N'-di-(4-pyridylmethyl) -1,2,4,5-benzenetetracarboxydiimide).[46] Zn(NDC)(DPMBI) exhibits selective CO_2 capture from flue gas.[46] An orthorhombic supercell of $1 \times 2 \times 2$ unit cells was taken as the simulation box and its dimensions were 25.915 Å × 28.3488 Å × 41.2084 Å. Here too, the TraPPE force field with LJ and charge sites[47] was considered for CO_2. While the gas-gas interactions included both LJ and Coulombic terms, that between the gas and the framework was treated using purely LJ interactions through the DREIDING[48] and UFF[44] force fields. Electrostatic interactions were calculated using Ewald summation method. Cross LJ parameters were calculated via the Lorentz-Berthelot mixing rule. Framework atoms were considered as frozen in their crystallographic positions. The force field parameters of framework atoms are provided in table S3. A cutoff radius of 12.8 Å was used for LJ interactions. The Peng-Robinson equation of state was used to convert pressure into chemical potential. In this case, the fugacity coefficients at a particular pressure and temperature were calculated using Thermosolver software.[49] We performed 4×10^7 cycles subsequent to 1×10^7 cycles which were devoted to equilibration.

2.2b *Perfluorinated Amorphous Polymer*: We had recently modelled the structure and gas adsorption characteristics of a conjugated microporous amorphous polymer based on tetraphenylethylene moieties.[50] In the current work, we examine theoretically the effect of perfluorinating this compound on its properties. The methodology adopted to create a model for this fluorinated compound is the same as that described in Ref.[50]. Further details are provided in Supplementary Information.

It is pertinent to note that the framework (adsorbent) has been treated to be rigid in the simulations reported

Table 1. Simulation details of CH_4 adsorption studies in FMOF-1 and $[Zn_2(L)]_\infty$ MOF. Both are orthorhombic systems.

MOF	Cell parameters	Simulation cell ccell	Temperature (K)
FMOF-1	a = b = 13.366 Å	2 × 2 × 1	288
$[Zn_2(L)]_\infty$ MOF	a = b = 7.025 Å	4 × 4 × 2	298

here. The organic linkers in MOF solids can in particular exhibit conformational flexibility which can modulate gas uptake. Introducing flexibility in the framework within the MCIN code is beyond the scope of the current manuscript. However, this aspect will be studied by us in future, using methods such as hybrid GCMC/MD.[51–55] Configurations were visualized using VMD.[56]

3. Results and Discussion

In order to assess whether the widely used generic force fields are able to describe the adsorbate-adsorbent interactions accurately, we have studied the adsorption of CO_2 in porous materials (two MOFs and one CMP) with both DREIDING and UFF force fields. Pair correlation functions have been calculated to delineate the intermolecular arrangements of adsorbed CH_4 and CO_2 as well as their favorable interaction sites within the MOF framework as a function of gas pressure. Specific structural details of the various MOFs are not described here as they can be obtained from the original literature.

3.1 *Adsorption Isotherm of CH_4*

3.1a *FMOF-1*: The adsorption isotherm calculated from MCIN is compared with experimental data[43] in figure 1a. To delineate the most favorable adsorption sites for CH_4 in the framework, pair correlation functions (PCFs) were calculated between the molecule and different sites of MOF. F-CH_4, N-CH_4, C-CH_4 and Ag-CH_4 PCFs were calculated at 1, 45 and 200 bar. PCFs for various sites at 1 bar (low pressure) are compared in figure 2a. Closest interactions for CH_4 were observed with the F atoms of the $–CF_3$, N and C atoms of the 1,2,4-triazole. Thus, further studies have been focused on these three interactions. The PCFs of CH_4 molecules around F, N, C of the MOF and other CH_4 molecules at 1 bar, 45 bar and 200 bar in figure S22a-c respectively. In figure S22a, three features at 3.5 Å, 4.3 Å, and 5.1 Å are seen. The first hump corresponds to the CH_4 interacting with a F atom of $–CF_3$ which is directed towards the pore and the remaining two correspond to the other two F atoms in the same CF_3 group. In figure S22b and c, the first hump corresponds to correlation between one of the N and C atoms of 1,2,4-triazole and the remaining correspond to other N and C atoms in the same group. We observe that although the relative magnitudes of the peaks are impacted by pressure, the peak positions are not. The peak heights increase with increasing pressure, as expected. The interactions exhibited by CH_4 with FMOF-1 atoms at 1 bar and 288 K are displayed in figure 2b.

3.1b $[Zn_2(L)]_\infty$ *MOF*: The adsorption isotherm of CH_4 simulated using MCIN is compared with experimental data[42] in figure 1b. Here too, PCFs are calculated to identify favorable interaction sites for CH_4 in MOF. The C-CH_4, H-CH_4 and O-CH_4 PCFs were calculated at 0.5 bar, 4 bar, 10 bar and 298 K and the same are compared at low pressure in figure 3a. The closest possible interactions for CH_4 are with the H and O atoms of 2, 2'-bipyridyl-5, 5'-dicarboxylic linker of the framework. We have compared PCFs and corresponding first shell coordination numbers of H-CH_4 as well as O-CH_4 at 0.5, 4 and 10 bar and at 298 K as shown in figure S23a–b. In figure S23a, the peak at 3.4 Å represents CH_4 interaction with the two H atoms of 2,2'-bipyridyl-5,5'- dicarboxylic group. In figure S23b, two prominent peaks centered at 3.6 Å and 6.0 Å are observed. The first one corresponds to the CH_4 interacting with the O atom of the carboxylate group of the linker. The second peak corresponds to CH_4 interacting with the O atoms of adjacent linker within the same pore. These interactions are depicted in figure 3b. The peak heights in the PCFs increase with increasing pressure, as expected. The number of CH_4 molecules near a H-atom of the MOF is around 1.1 at a pressure of 45

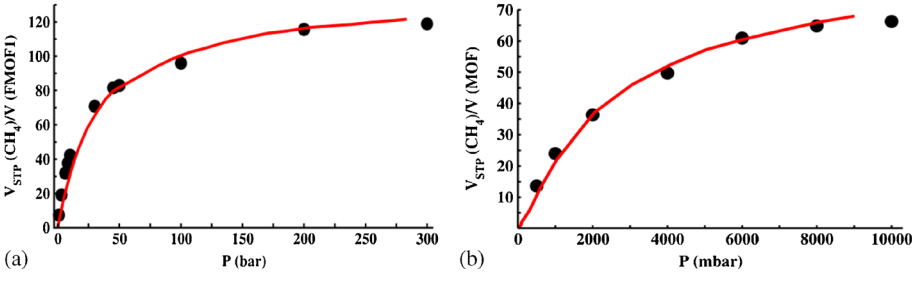

Figure 1. Comparison of adsorption isotherm of CH_4 in a) FMOF-1; and b) $[Zn_2(L)]_\infty$ MOF obtained from MCIN (black circles) at 288 K and 298 K with experimental data (continuous line).[42,43]

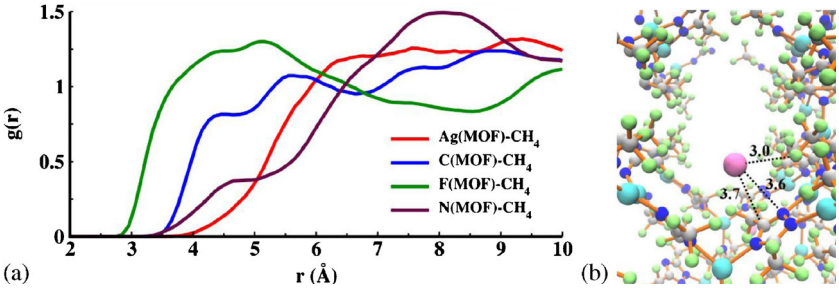

Figure 2. a) Comparison of pair correlation functions between different types of atoms of FMOF-1 and CH_4 at 1 bar and 288 K. b) Primary interactions for CH_4 in FMOF-1 at 1 bar and 288 K. Distances are in Å unit. Color scheme: C-silver, H-lime, N-blue, Ag-cyan and CH_4-mauve.

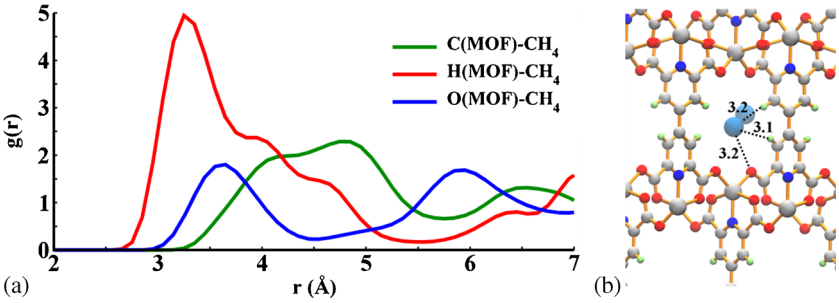

Figure 3. a) Comparison of the pair correlation functions between different types of atoms of $[Zn_2\ (L)]_\infty$MOF and CH_4 at 0.5 bar and 298 K. b) Primary interactions for CH_4 in the $[Zn_2(L)]_\infty$ MOF at 0.5 bar and 298 K. Distances are in Å unit. Color scheme: C-silver, H-lime, O-red, and CH_4-iceblue.

bar and does not increase much further with increase in pressure.

3.2 *Adsorption Isotherms of CO_2*

3.2a *IRMOF-1*: Simulations in this MOF were carried out to validate the MCIN code, as described in Supplementary Information. The calculated adsorption isotherm of CO_2 at 298 K is compared in figure S8 with the simulation results of Snurr et al.,[57] and the isotherms determined from experiment.[57] Figure S8 shows that the predicted uptake using LJ interactions alone is considerably lower than the experimental result. Inclusion of coulombic interactions between the gas molecules is able to estimate the saturated loading in much better agreement with experiment. More importantly, it captures the inflection behavior. Our GCMC results agree well with those of Snurr and coworkers.[57] It should be noted that the inflection is captured without invoking any charges in the MOF structure itself. Figure S8 clearly shows the importance of electrostatic interactions between CO_2 molecules to reproduce the shape of the experimental adsorption isotherm. The marginal difference with experimental CO_2 uptake could be due to (i) deficiencies in the potential, (ii) the morphology of the experimental MOF sample may impose a kinetic barrier which can result in a lower uptake than the theoretical estimate.[58]

The intermolecular arrangement of adsorbed CO_2 molecules as well as favorable interaction sites for CO_2 with the IRMOF-1 have been studied based on PCFs between different pairs of atoms. Several PCFs were calculated at 298 K and 4, 10 and 20 atm. The intermolecular PCFs between adsorbed CO_2 molecules at three pressures are shown in figure 4. The peak heights of $g_{C-C}(r)$ and $g_{C-O}(r)$ increase with increasing pressure. Based on the PCFs of CO_2 with MOF atoms obtained at low pressure (4 atm), the following interactions can be identified between adsorbed CO_2 and IRMOF-1: (i) O of CO_2 and H of the phenyl rings of IRMOF-1 (weak hydrogen bond interaction), (ii) C of CO_2 and O of carboxylate groups of IRMOF-1 (Lewis acid-base interaction), and (iii) center of mass of phenyl rings and the C atom of the CO_2(π-π interaction). Given the absence of electronic degrees of freedom in our simulations, these interactions have been identified on established geometric criteria alone.[59–62] These PCFs have been calculated at 4, 10 and 20 atm and are shown in figure 5a–c. In figure 5a, two peaks

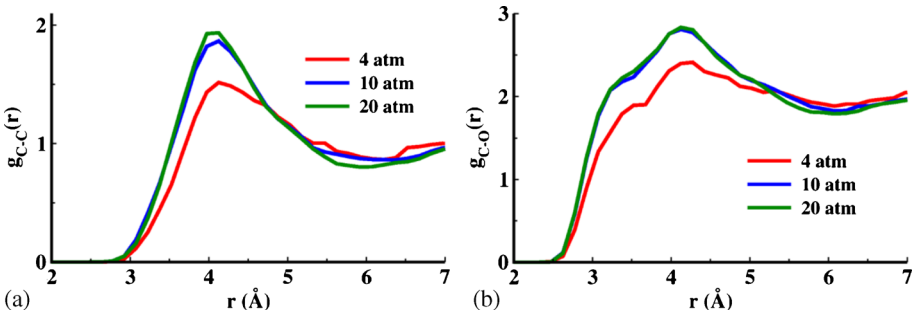

Figure 4. Intermolecular pair correlation functions between sites of adsorbed CO_2 molecules in IRMOF-1 a) C-C and b) C-O at 298 K and 4 atm, 10 atm, and 20 atm.

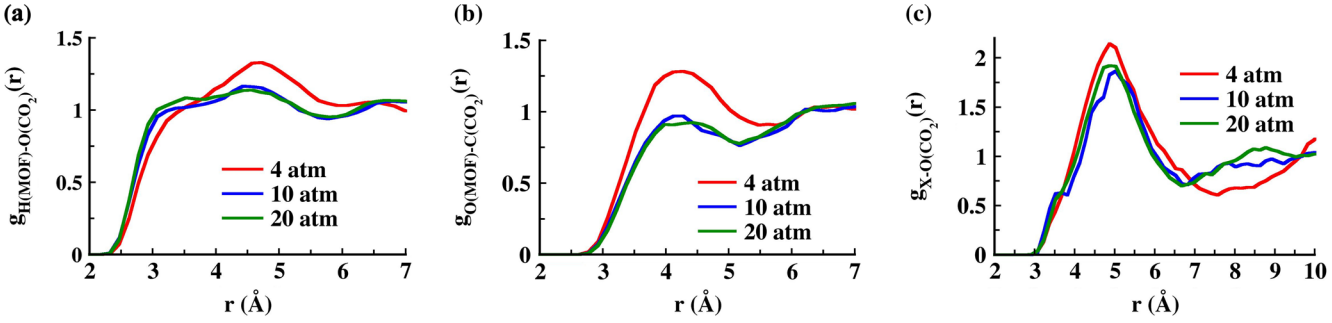

Figure 5. Pair correlation functions between a) H of MOF and O of CO_2; b) O of MOF and C of CO_2; and c) center of mass of phenyl ring (X) and O of CO_2 at 298 K and 4 atm, 10 atm, and 20 atm. The MOF is IRMOF-1.

can be found at 3.2 Å and 4.6 Å. The first one corresponds to the interaction of O of CO_2 with one of the H of phenyl ring while the other corresponds to the interaction of CO_2 with the other H of the adjacent phenyl ring within the same pore. In figure 5b, the peak at 4.2 Å corresponds to the C of CO_2 interacting with the O of carboxylate group of IRMOF-1. Although the coordination number increases with pressure (as it should), the magnitude of the peak (which is the probability density) decreases with increasing pressure. At higher pressures, CO_2 prefers to adsorb in the pores by interacting with H of phenyl rings which is the entropically dominant zone.[63] The first shell coordination number of C of CO_2 around the O of carboxylate group of IRMOF-1 as a function of pressure is plotted in figure S24. This behavior is analogous to the adsorption isotherm (blue curve in figure S8). The number of CO_2 molecules present near O of carboxylate group of IRMOF-1 at 12 atm is 2.7 and does not change much, with increase in gas pressure. In figure 5c, the peak at 5 Å corresponds to the π-π interaction between phenyl ring of IRMOF-1 and CO_2. Here too, the peak height decreases with increasing pressure as CO_2 prefers to adsorb in the entropically dominant site. The interactions between CO_2 and IRMOF-1 are shown in figure 6.

3.2b *Zn(NDC)(DPMBI) MOF*: Here, NDC = 2,7-naphthalene dicarboxylate, and DPMBI = N,N'-di-(4-pyridylmethyl)-1,2,4,5-benzenetetracarboxydiimide). The adsorption isotherm of CO_2 in this MOF calculated from MCIN is compared against experimental data[46] in figure 7. Here too, the intermolecular arrangement of adsorbed CO_2 molecules as well as the favorable interaction sites of CO_2 with the Zn(NDC)(DPMBI) MOF have been examined. Several PCFs have been calculated at 298 K and 0.05, 0.4 and 0.8 atm. Intermolecular PCFs between adsorbed CO_2 molecules at three pressures are shown in figure 8. The peak magnitude of $g_{C-C}(r)$, $g_{C-O}(r)$ and corresponding coordination numbers increase with increasing pressure. At 0.8 atm pressure, around 1.2 CO_2 molecules are observed in the first coordination shell of any CO_2 molecule. Based on MOF-CO_2 PCFs obtained at the lowest pressure (0.05 atm), the following favorable interactions between adsorbed CO_2 and Zn(NDC)(DPMBI) are identified: i) O of CO_2 and H of the NDC linker of the MOF (weak hydrogen bonding), ii) C of CO_2 and O of carboxylate groups of linker (Lewis acid-base interaction), and iii) center of mass of pyridine rings and the O of the CO_2 (π-π interaction). As before, these interactions have been identified on established

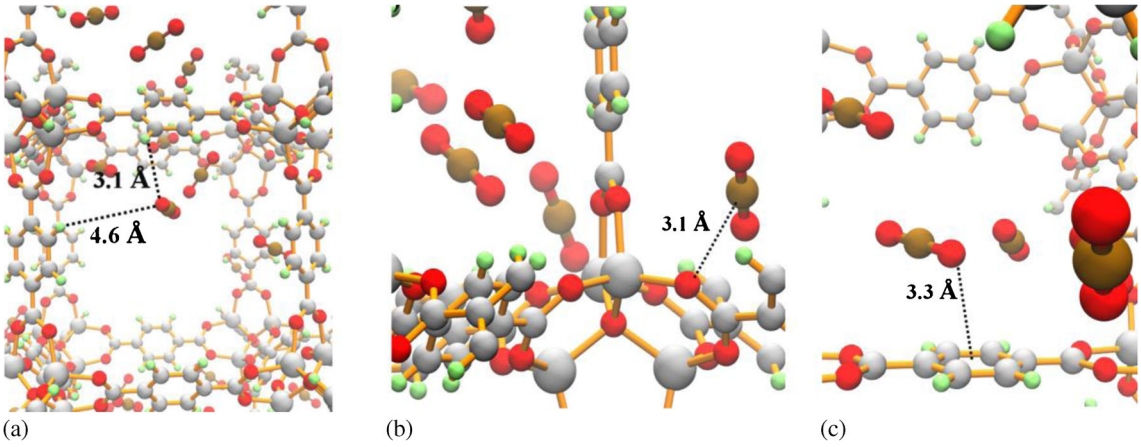

Figure 6. Interactions between a) H of MOF and O of CO_2; b) O of MOF and C of CO_2; and c) center of mass of phenyl ring and O of CO_2 at 298 K and 4 atm in IRMOF-1. Color scheme: MOF atoms: C-Silver, O-red, H-green, Zn-iceblue and CO_2: C-tan and O-red.

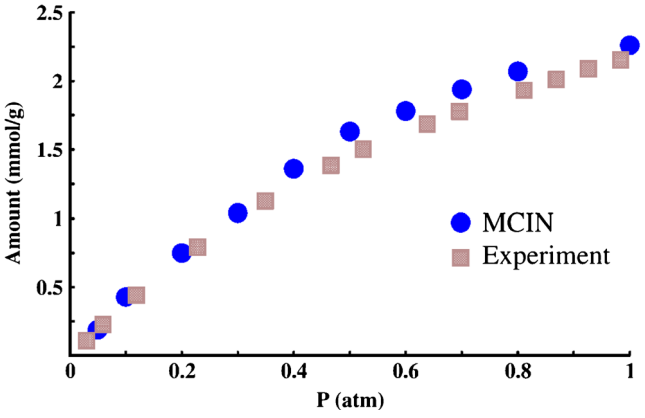

Figure 7. Adsorption isotherms of CO_2 in Zn(NDC)(DPMBI) at 298 K calculated through MCIN (blue circles) compared with experimental (brown squares) data.[46]

geometric criteria alone.[59–62] The corresponding PCFs have been calculated at 0.05, 0.4 and 0.8 atm and are shown in figure 9a–c. In figure 9a, the peak at 3.2 Å corresponds to the interaction of O of CO_2 with one of the H of NDC linker ring. In figure 9b, the peak at 4.2 Å corresponds to the C of CO_2 interacting with the O of the carboxylate group of linkers (NDC or DPMBI) via Lewis acid-base interactions. In figure 9b, the peak height increases with pressure unlike the behavior seen in IRMOF-1 (figure 5b). In Zn(NDC)(DPMBI) MOF, O of carboxylic groups are directed towards the pore which is the entropically dominant region.[63] Thus, CO_2 prefers this location at high pressures. However, in IRMOF-1, O of carboxylate groups are at the corners of the pores which is the energetically favorable domain. Thus, at high pressures, CO_2 prefers to bind in the entropically dominant region and the peak height decreases with increasing pressure (figure 5b). In figure 9c, the peak at 5 Å corresponds to π-π interaction between the pyridine ring of DPMBI and CO_2. These interactions between CO_2 and the framework atoms can be visualized in figure 10.

3.2c *Perfluorinated Conjugated Microporous Polymer*: MD simulations using a force field were carried out on a model compound, fluorine substituted tetraphenylethylene

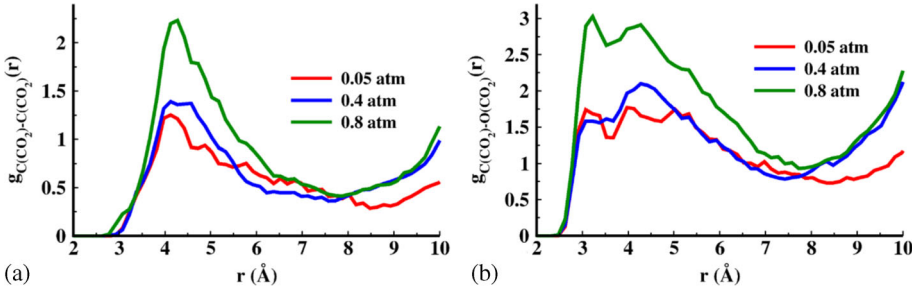

Figure 8. Intermolecular pair correlation functions between sites of adsorbed CO_2 molecules in Zn(NDC)(DPMBI) MOF a) C-C; and b) C-O at 298 K and 0.05 atm, 0.4 atm, and 0.8 atm.

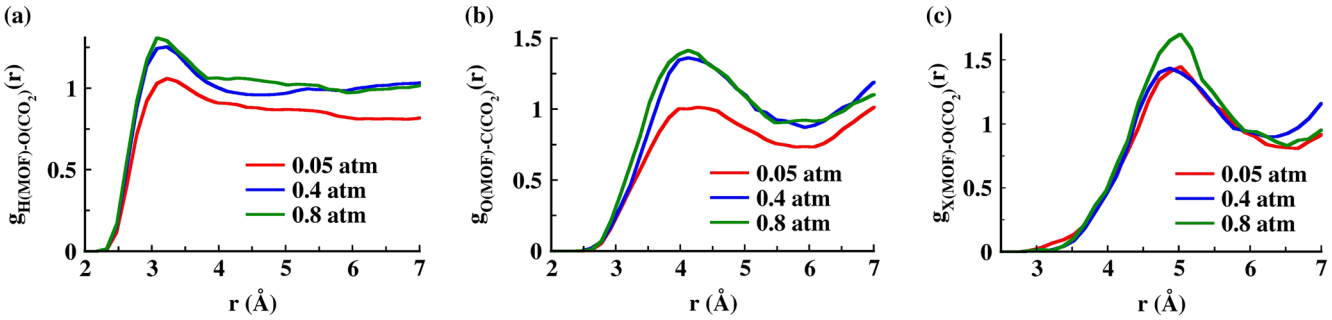

Figure 9. Pair correlation functions between a) H of MOF and O of CO_2; b) O of MOF and C of CO_2; and c) center of mass of pyridine ring (X) and O of CO_2 at 298 K and different pressures: 0.05 atm, 0.4 atm, and 0.8 atm. The MOF is Zn(NDC)(DPMBI) MOF.

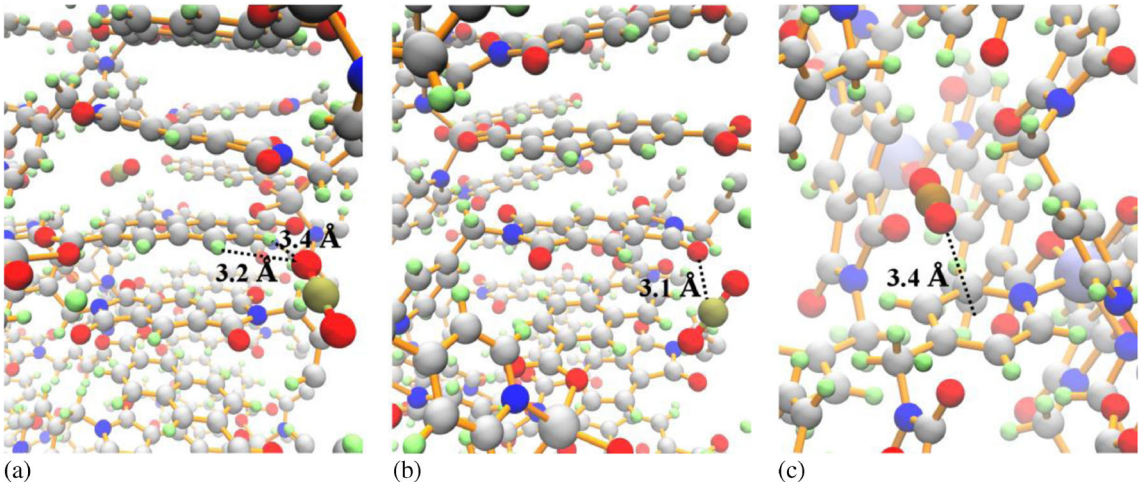

Figure 10. Interactions between a) H of MOF and O of CO_2; b) O of MOF and C of CO_2; and c) center of mass of pyridine ring and O of CO_2 at 298 K and 0.05 atm in Zn(NDC)(DPMBI) MOF. Color scheme: MOF atoms: C-silver, O-red, H-green, Zn-iceblue and CO_2: C-tan, O-red.

based conjugated microporous polymer, TPE-FCMP (**1**) as discussed in Supporting Information. **1** was characterized through calculations of powder X-ray diffraction (PXRD), accessible surface area (ASA) and adsorption isotherm of CO_2. The density of the initial model obtained using MD simulations is 1.1 g/cc. The accessible surface area of this model structure was calculated using a Monte Carlo code developed by Snurr and co-workers.[64] Employing a value of 3.681 Å for the probe diameter of N_2, the ASA for the 1.1 g/cc CMP model was calculated to be 481 m^2/g. In general, CMPs are kinetically controlled structures and do not show long range periodicity, unlike MOFs and covalent organic frameworks (COFs).[65–67] In our earlier work on TPE-CMP, the density of the modelled structure was decreased by 20% in order to match the accessible surface area[50] determined experimentally. The same procedure was applied herein to TPE-FCMP. The density of **1** was decreased to 0.89 g/cc, in steps. At each step, post energy minimization, MD simulations for over 2 ns was carried out and subsequently, the ASA was recalculated. The calculated ASA of the structure at 0.89 g/cc density was found to be 867 m^2/g. The PXRD pattern of the 0.89 g/cc structure was calculated (see Supplementary Information for more details) with a resolution of 0.11 $Å^{-1}$ and is shown in figure S16. One of the oligomer in TPE-FCMP is highlighted in figure S14. To understand the connectivity among the pores and void spaces, N_2 accessible surface (with a probe radius of 1.82 Å)[68] was estimated using Mercury[69] and the same is shown in figure 11a, where the void space architecture in the polymer is shown in yellow. The total void volume is estimated to be about 36% of the simulation cell.

3.2d *GCMC simulations of CO_2 in **1***: GCMC simulation results reported here were carried out using MCIN,[70,71] as discussed in section S4 of Supporting Information. In our simulations, both the polymer and

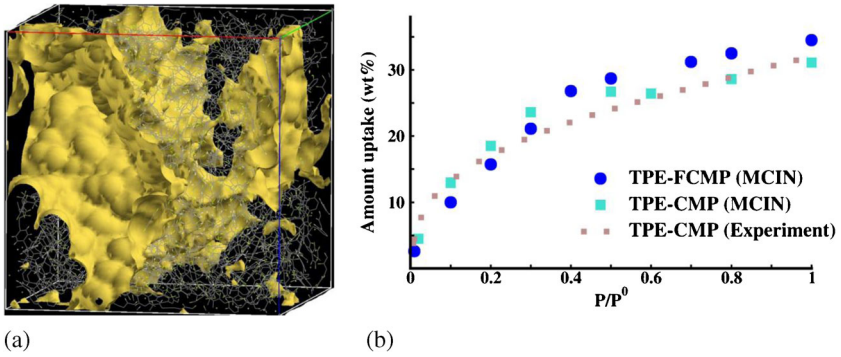

Figure 11. a) Pore architecture in model TPE-FCMP. Yellow region indicates the void space for N_2 while C and H atoms of the polymer are in grey and white colors respectively. b) Adsorption isotherms for CO_2 in conjugated microporous polymers at 195 K. Experimental data for TPE-CMP[50] (brown dotted line); Blue circles and cyan squares are results from MCIN in TPE-FCMP and TPE-CMP respectively.

CO_2 were assumed to be rigid. The calculated adsorption isotherm of CO_2 in TPE-FCMP (**1**), TPE-CMP and the latter's experimental uptake[50] are compared in figure 11b. Our calculations predict a 10% increase in the uptake of CO_2 in the perfluorinated polymer over its hydrogenated counterpart.

Adsorption isotherms of CO_2 in IRMOF-1 (298 K), Zn(NDC)(DPMBI) (298 K) and TPE-CMP (195 K) calculated using both DREIDING and UFF force fields (for the adsorbent) are presented in figures S9, S10 and S15, respectively. Experimentally determined isotherms are also provided. The amount of CO_2 uptake calculated using the UFF force field for the adsorbent is marginally higher than that of either the DREIDING prediction or experiment.

To understand the arrangement of adsorbed CO_2 molecules near the nodes as well as linkers in the TPE-FCMP polymer, their spatial distribution in the matrix was studied at three pressures: 0.1, 0.5 and 1.0 atm. In typical MOF simulations, such spatial density maps are averaged over ensemble and time. However, all the nodes and linkers are not present in the same environment in **1**. It lacks long range periodicity and nodes or linkers line present along the pore surface have a different environment than those lying in the core of the polymer matrix. Thus, we have chosen to examine the locations of CO_2 around a specifically chosen tetraphenylethene (node) and a 4,4'-diethynyloctafluorobiphenyl (linker) moiety which were identified visually to lie on a pore surface. These were obtained via constant-NVT MD simulations carried out for 15 ns each at a temperature of 195 K in a fixed polymer framework. Isosurfaces of CO_2 density with respect to either the node or the linker present on the pore surface are displayed in figure 12a–f. The cheese colored region indicates the distribution of CO_2. The maps demonstrate that CO_2 interacts with the phenyl and ethylenic groups of the node and with the phenyl and acetylenic groups of the linker.

3.3 *Comparison of GCMC results with MD simulations*

Results from MCIN, in terms of adsorption isotherms were compared against experimental data above. Neutron and X-ray scattering experiments can provide information on intermolecular structure of molecules adsorbed in MOF solids. However, these experiments are challenging and thus are very rare.[72–74] Thus, we compare the intermolecular structure obtained from MCIN against results from MD simulations. A key quantity to characterize is the pair correlation function, results of which are presented here.

In these simulations, DREIDING and TraPPE force fields were used to model the IRMOF-1 and CO_2 in their all-atom representations respectively. CO_2-CO_2 structural correlations were calculated at a pressure of 10 atm. At this pressure, the variation in the number of adsorbed CO_2 molecules with MC cycles is shown in figure S25. The number of CO_2 molecules fluctuate around a mean value of 86. CO_2 -CO_2 pair correlation functions obtained from MD simulations performed with 86 molecules in the MOF did not quite match those obtained from the GCMC simulations. The issue was resolved to the fact that the GCMC run had significant fluctuations in the number of molecules while the MD run was performed in the canonical ensemble. Needless to state, the difference is a consequence of the fact that one is not in the thermodynamic limit. We

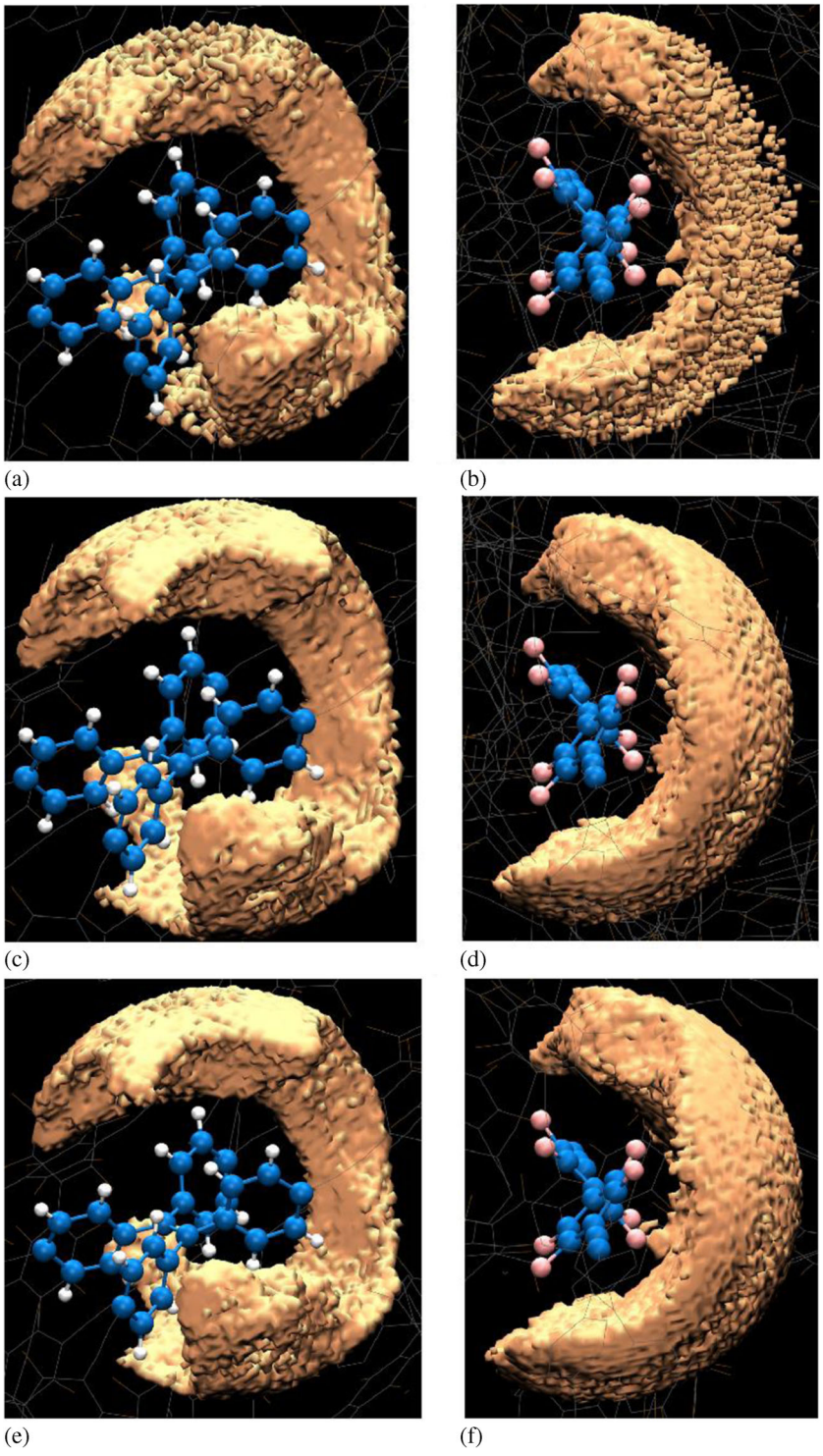

Figure 12. (a, c, e/b, d, f) Spatial density distribution maps of CO_2 around a specific node and linker in TPE-FCMP at 195 K around a specific node/linker at 0.1, 0.5 and 1.0 atm respectively. Cheese colored surfaces show possible locations of CO_2 at an isosurface value of 5×10^{-4} a.u. Blue and tan colors are C and H atoms of the node and the linkers in the polymer respectively. Rest of the CMP atoms are shown as thin lines.

obtained the probability distribution (histogram) of the number of molecules from the GCMC simulation and performed six independent MD simulations, each in the NVT ensemble but with different number of molecules ranging between 60 and 120. Pair correlation functions obtained from each of these runs were weighted (via

the histogram obtained from the GCMC run) and a mean pair correlation function was obtained which is compared to that from the GCMC run in figure S17a–d. They match rather well, giving confidence on the configurational sampling in MCIN.

Furthermore, we characterized the vibrational, orientational and diffusive properties of CO_2 molecules in IRMOF-1. Low frequency infrared spectrum provides a precise understanding on the nature of interaction between probe molecules e.g., CO, NO, and CO_2, etc., with the MOF.[75] Herein, vibrational density of states were calculated to delineate the intermolecular modes of adsorbed CO_2 in IRMOF-1.

3.3a *Vibrational density of states*: The vibrational density states (VDOS) have been calculated to understand intermolecular 'modes' of adsorbed CO_2 in IRMOF-1 at 10, 20 and 30 atm and 298 K. Details of the calculations are provided in Supplementary Information. The low frequency band to intermolecular 'modes' exhibits a blue shift with increasing pressure which is shown in figure S18.

A key character of adsorbed gases in framework solids is cooperativity. Although in general the isosteric heat of adsorption decreases with increasing coverage, under certain circumstances, it can show an increase (followed by a decrease). This occurs due to favorable interaction between the adsorbed gas molecules, a feature called as cooperativity in the literature.[76,77] Cooperativity between CO_2 adsorbed in IRMOF-1 was studied by examining the intermolecular angle distribution between neighboring molecules at 298 K and 10 atm. This distribution was compared with that obtained from bulk CO_2. Molecules confined within narrow pores, with pore widths of a few molecular diameters, can exhibit a wide range of physical behavior.[78,79] The introduction of wall forces, and the competition between fluid-wall and fluid-fluid forces, can lead to interesting surface-driven phase changes.[80–84] These include new kinds of phase transitions not found in the bulk phase. Recently, Snurr *et al*., have calculated the density of CO_2 in IRMOF-1 and compared the same with that of bulk CO_2 at 298 K.[57] However, the orientational distribution between adsorbed CO_2 molecules has not been studied yet, to our knowledge.

3.3b *CO_2 orientation*: The orientational ordering between near neighbour adsorbed CO_2 molecules in IRMOF-1 was calculated from the configurations obtained from MCIN at 298 K and 10 atm. An illustration of a typical near-neighbour configuration is shown in figure 13. To aid further discussion, we provide the following nomenclature. The probability distributions of the angle was calculated between $\overrightarrow{O_pO_q}$ and $\overrightarrow{C_2O_a}$, where O_a is the closest oxygen atom to the central carbon C_2. The analysis has been carried out for molecules lying within a distance of 3.4 Å which defines the first coordination shell as seen from the C-O $g_{CO}(r)$ in fluid CO_2.[85]

Simultaneously, for the sake of comparison, classical NVT-MD simulations of bulk CO_2 were carried out using LAMMPS[86] with a time step of 1 ns at 298 K. The EPM2[87] potential model was employed for CO_2. A good match between the $g_{CO}(r)$ of bulk CO_2 and that in the IRMOF-1 (via MCIN) was obtained at a bulk density of 1.1 g/cc as shown in figure S21. The probability distribution of angles between the vectors $\overrightarrow{O_pO_q}$ and $\overrightarrow{C_2O_a}$ was calculated. A comparison between the data in bulk CO_2 and that confined in IRMOF-1 is displayed in figure 13. The distributions in figure 13

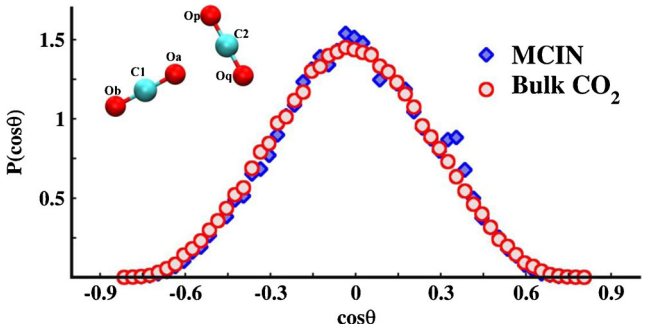

Figure 13. Probability distribution of angles between $\overrightarrow{O_pO_q}$ and $\overrightarrow{C_2O_a}$ (Inset) obtained for CO_2 in IRMOF-1 from MCIN and from MD simulations of bulk CO_2 at 298 K and 1.1 g/cc. Inset: Illustration of a typical near-neighbor arrangement of CO_2 molecules. The carbon of the central molecule is denoted as C2 and the oxygen atom from another molecule closest to it is denoted as Oa.

Table 2. Self-diffusion coefficients of CO_2 in IRMOF-1 at 298 K.

Pressure (atm)	Diffusion Coefficient ($\times 10^{-8}$ m^2/s)
10	6.8
20	3.9
30	3.1

Table 3. Self-diffusion coefficients of CO_2 in TPE-FCMP at 195 K.

Pressure (atm)	Diffusion Coefficient ($\times 10^{-9}$ m^2/s)
0.1	1.3
0.5	1.0
1.0	0.7

exhibit a preference for cosθ values around zero indicating that the closest neighboring molecules prefer a distorted T-shaped configuration. This feature in the near-neighbour arrangement between CO_2 neighbors is comparable between the adsorbed and bulk phases.

Diffusion behavior of gases is of paramount importance in many applications that are envisioned for porous materials.[14,88–92] The self-diffusion coefficients of CO_2 have been studied in IRMOF-1 as well as TPE-FCMP at various pressures. Details of the calculations are provided in Supporting Information. As expected, the diffusion coefficients of CO_2 decrease with increasing pressure, and these are shown in tables 2 and 3.

4. Conclusions

Adsorption isotherms for CO_2 in many metal organic framework solids obtained from GCMC simulations were presented here. The calculated isotherms compare very well with experimentally determined ones, up to 1 atm pressure. Intermolecular structural correlations between the CO_2 molecules present within their micropores were also investigated. They exhibited considerable similarities with those observed in bulk fluid CO_2. Specific sites of adsorption existing in metal organic framework solids with which CO_2 interacts have been identified. These include: fluorine, phenyl and carboxylate groups. van der Waals, Lewis acid-base, weak hydrogen bonding and π-π interactions determine the adsorption of CO_2 in these solids; this understanding can aid in the design of other novel architectures involving such functional groups. Apart from the surface chemistry of the pores, the pore architecture too determines gas uptake, as exemplified by differences in the dependence of $g_{CO2-O}(r)$ on pressure in two MOFs studied here. Such pair correlation functions can in principle be obtained through neutron scattering experiments and we hope our work would spur more efforts in this area.[73,74,93–95]

We have also been able to predict the uptake of CO_2 in a model microporous, amorphous polymer. Perfluorination is shown to increase CO_2 uptake by at least 10%. It remains to be seen if this perfluorinated polymer can be synthesized and its CO_2 uptake be measured for a comparison to the simulation results presented here. The closest interaction sites for CO_2 in this polymer are located at the pore surface lined by the linkers.

For the systems studied here, the UFF force field (for the adsorbent) predicts a marginally higher gas uptake than that obtained from the DREIDING force field. The latter is able to quantitatively reproduce experimentally determined isotherms. The current Monte Carlo simulations have been performed within a rigid framework approximation. However, organic linkers in MOFs can in particular show some degree of conformational flexibility which can modulate gas uptake at ambient conditions.[21] In the systems studied herein, the absence of flexibility of the framework appears not to influence amount of gas adsorption. Yet, we plan to implement methods to introduce flexibility to the adsorbent within MCIN, in future.[96]

We are interested in predicting model MOF compounds which are not only CO_2-philic but are also stable in the presence of water vapor. This aspect will constitute our future endeavours.

Supplementary Information

The Supplementary Information associated with this article has sections containing the development of MCIN code and applications of MCIN: validation of MCIN by reproducing simulated and experimental adsorption isotherms, modelling CO_2 adsorption in TPE-FCMP, comparison of pair correlation functions of CO_2 with respect to MOF sites obtained from MCIN and LAMMPS, vibrational density of states of CO_2 in IRMOF-1 and CO_2 diffusion in IRMOF-1 and TPE-FCMP at various pressures, comparison of pair correlation functions of adsorbed CO_2 with bulk CO_2, comparison pair correlation functions of CH_4 in FMOF-1 and $[Zn_2(L)]_\infty$ at various pressures and running coordination number of CO_2 around carboxylate group of IRMOF-1. The Supplementary Information for this article is available at http://www.ias.ac.in/chemsci.

Acknowledgements

We thank DST for support. The first author acknowledges CSIR for a research fellowship. The second author acknowledges SSL for a Senior Fellowship. We thank Prof. Tapas Kumar Maji and his research group at JNCASR for many insightful discussions.

References

1. Düren T, Bae Y-S and Snurr R Q 2009 *Chem. Soc. Rev.* **38** 1237
2. Rowsell J L C, Millward A R, Park K S and Yaghi O M 2004 *J. Am. Chem. Soc.* **126** 5666
3. Getman R B, Miller J H, Wang K and Snurr R Q 2011 *J. Phys. Chem. C* **115** 2066
4. Kumar A V A, Jobic H and Bhatia S K 2006 *J. Phys. Chem. B* **110** 16666
5. Siriwardane R V, Shen M S and Fisher E P 2003 *Energy Fuels* **17** 571

6. Economides M J and Wood D A 2009 *J. Nat. Gas Sci. Eng.* **1** 1
7. Wang W, Ma C, Lin P, Sun L and Cooper A I 2013 *Energy Environ. Sci.* **6** 105
8. Prajwal B and Ayappa K 2014 *Adsorption* **20** 769
9. Arenillas A, Smith K, Drage T and Snape C 2005 *Fuel* **84** 2204
10. Haldar R, Narayan R, Pradeep R and Maji T K 2012 *Indian J. Chem., Sec A* **51A** 1231
11. Myers A and Monson 2014 *Adsorption* **20** 591
12. Belmabkhout Y, Frére M and Weireld G D 2004 *Meas. Sci. Technol.* **15**
13. Nakashima M, Shimada S, Inagaki M and Centeno T 1995 *Carbon* **33** 1301
14. Bao Z, Yu L, Ren Q, Lu X and Deng S 2011 *J. Colloid Interface Sci.* **353** 549
15. Fischer M and Bell R G 2012 *J. Phys. Chem. C* **116** 26449
16. Liu Z, Horikawa T, Do D and Nicholson D 2012 *J. Colloid Interface Sci.* **368** 474
17. Torrisi A, Bell R G and Mellot-Draznieks 2010 *Cryst. Growth Des.* **10** 2839
18. Naumov S, Valiullin R, Kaürger J and Monson P 2009 *Phys. Rev. E* **80** 031607
19. Mowat J P S, Seymour V R, Griffin J M, Thompson S P, Slawin A M Z, Fairen-Jimenez D, Düren T, Ashbrook S E and Wright P A 2012 *Dalton Trans.* **41** 3937
20. Chen L, Grajciar L, Nachtigall P and Düren T 2011 *J. Phys. Chem. C* **115** 23074
21. Kanoo P, Reddy S K, Kumari G, Haldar R, Narayana C, Balasubramanian S and Maji T K 2012 *Chem. Commun.* **48** 8487
22. Yang Q, Liu D, Zhong C and Li J R 2013 *Chem. Rev.* **113** 8261
23. Purton C J and Parker S 2013 *Mol. Simul.* **39** 1240
24. Dubbeldam D, Torres-Knoop A and Walton K S 2013 *Mol. Simul.* **39** 1253
25. Nicholson D and Parsonage N G 1982 In *Computer simulation and the statistical mechanics of adsorption* (Academic Press: London)
26. Esselink K, Loyens L D J C and Smit B 1995 *Phys. Rev. E* **51** 1560
27. Bates S P, Van Well W J M, Van Santen R A and Smit B 1997 *Mol. Simul.* **19** 301
28. Smit B and Krishna R 2001 *Curr. Opin. Solid State Mater. Sci.* **5** 455
29. Kim J and Smit B 2012 *J. Chem. Theory Comput.* **8** 2336
30. Snurr R Q, Bell A T and Theodorou D N 1993 *J. Phys. Chem.* **97** 13742
31. Severson B L and Snurr R Q 2007 *J. Chem. Phys.* **126** 134701
32. Kowalczyk P, Tanaka H, Kaneko K, Terzyk A P and Do D D 2005 *Langmuir* **21** 5639
33. Rahimi M, Singh J K, Babu D J, Schneider J J and Müller-Plathe F 2013 *J. Phys. Chem. C* **117** 13492
34. Liu J C and Monson P A 2006 *Ind. Eng. Chem. Res.* **45** 5649
35. Malani A and Ayappa K G 2009 *J. Phys. Chem. B* **113** 1058
36. Channon Y M, Catlow C R A, Gorman A M and Jackson R A 1998 *J. Phys. Chem. B* **102** 4045
37. Martin M G 2013 *Mol. Simul.* **39** 1212
38. Kofke D A and Mihalick B C 2002 *Fluid Phase Equilib.* **194–197** 327
39. Jorgensen W L and Tirado-Rives J 2005 *J. Comput. Chem.* **26** 1689
40. Gupta A, Chempath S, Sanborn M J, Clark L A and Snurr R Q 2003 *Mol. Simul.* **29** 29
41. Yang C, Kaipa U, Mather Q Z, Wang X, Nesterov V, Venero A F and Omary M A 2011 *J. Am. Chem. Soc.* **133** 18094
42. Lin X, Blake A, Wilson J C, Sun X Z, Champness N R, George M W, Hubberstey P, Mokaya R and Schröder M 2006 *J. Am. Chem. Soc.* **128** 10745
43. Nijem N, Canepa P, Kaipa U, Tan K, Roodenko K, Tekarli S, Halbert J, Oswald I W H, Arvapally R K, Yang C, Thon- hauser T, Omary M A and Chabal Y J 2013 *J. Am. Chem. Soc.* **135** 1261
44. Rappe A K, Casewit C J, Colwell K S, Goddard W A and Skiff W M 1992 *J. Am. Chem. Soc.* **114** 10024
45. Martin M G and Siepmann J I 1998 *J. Phys. Chem. B* **102** 2569
46. Leong C F, Faust T B, Turner P, Usov P M, Kepert C J, Babarao R, Thornton A W and D'Alessandro D M 2013 *Dalton Trans.* **42** 9831
47. Potoff J J and Siepmann J I 2001 *AIChE J.* **47** 1676
48. Mayo S L, Olafson B D and Goddard W A 1990 *J. Phys. Chem.* **94** 8897
49. Barnes C 2006 In *ThermoSolver: An Integrated Educational Thermodynamics Software Program*. H.B.S. thesis (Oregon State University Library, Special Collections: Oregon, USA) p. 12
50. Suresh V M, Bonakala S, Roy S, Balasubramanian S and Maji T K 2014 *J. Phys. Chem. C* **118** 24369
51. Greathouse J A, Kinnibrugh T L and Allendorf M D 2009 *Ind. Eng. Chem. Res.* **48** 3425
52. Skoulidas A I and Sholl D S 2005 *J. Phys. Chem. B* **109** 15760
53. Wongsinlatam W and Remsungnen T 2013 *J. Chem.* **2013** 1
54. Ghoufi A and Maurin G 2010 *J. Phys. Chem. C* **114** 6496
55. Krokidas P, Skouras E, Nikolakis V and Burganos V 2008 *Mol. Simul.* **34** 1299
56. Humphrey W, Dalke A and Schulten K 1996 *J. Mol. Graph* **14** 33
57. Walton K S, Millward A R, Dubbeldam D, Frost H, Low J J, Yaghi O M and Snurr R Q 2008 *J. Am. Chem. Soc.* **130** 406
58. Mehio N, Dai S and Jiang D E 2014 *J. Phys. Chem. A* **118** 1150
59. Derewenda Z S, Lee L and Derewenda U 1995 *J. Mol. Biol.* **252** 248
60. Gautham R D and Thomas S 2001 In *The Weak Hydrogen Bond: In Structural Chemistry and Biology* (Oxford University Press: London)
61. Hunter C A and Sanders J K M 1990 *J. Am. Chem. Soc.* **112** 5525
62. Baburin I A, Blatov V A, Carlucci L, Ciani G and Proserpio D M 2008 *Cryst. Eng. Comm.* **10** 1822
63. Suraweera N S, Albert J R, Barnes C E and Keffer D J 2014 *Int. J. Hydrogen Energy* **39** 9241
64. Düren T, Sarkisov L and Snurr R Q 2007 *Research section calculating the accessible surface area for non-orthorhombic unit cells* (http://people.bath.ac.uk/td222/research/surface_area/non_ortho/index.html)

65. Budd P M, Ghanem B S, Makhseed S, McKeown N B, Msayib K J and Tattershall C E 2004 *Chem. Commun.* 230
66. Jiang J -X, Su F, Trewin A, Wood C D, Niu H, Jones J T A, Khimyak Y Z and Cooper A I 2008 *J. Am. Chem. Soc.* **130** 7710
67. Wu P, Wang J, He C, Zhang X, Wang Y, Liu T and Duan C 2012 *Adv. Funct. Mater.* **22** 1698
68. Jiang J -X, Trewin A, Su F, Wood C D, Niu H, Jones J T A, Khimyak Y Z and Cooper A I 2009 *Macromolecules* **42** 2658
69. Macrae C F, Edgington P R, McCabe P, Pidcock E, Shields G P, Taylor R, Towler M and van de Streek J 2006 *J. Appl. Crystallogr.* **39** 453
70. Allen P and Tildesley D 1987 In *Computer simulation of liquids* (Oxford science publications, Clarendon Press: New York)
71. Frenkel D and Smit B 2001 In *Understanding Molecular Simulation: From Algorithms to Applications* 2nd Edition (Academic Press: London)
72. Dubbeldam D, Frost H, Walton K S and Snurr R Q 2007 *Fluid Phase Equilib.* **261** 152
73. Queen W L, Bloch E D, Brown C M, Hudson M R, Mason J A, Murray L J, Ramirez-Cuesta A J, Peterson V K and Long J R 2012 *Dalton Trans.* **41** 4180
74. Wu H, Simmons J M, Srinivas G, Zhou W and Yildirim T 2010 *J. Phys. Chem. Lett.* **1** 1946
75. Daturi M 2012 *Curr. Phys. Chem.* **2** 178
76. Vaidhyanathan R, Iremonger S S, Shimizu G K H, Boyd P G, Alavi S and Woo T K 2012 *Angew. Chem., Int. Ed.* **51** 1826
77. Kitagawa S and Matsuda R 2007 *Coord. Chem. Rev.* **251** 2490
78. Das C K and Singh J K 2013 *J. Chem. Phys.* **139** 174706
79. Liu Z, Do D and Nicholson D 2011 *J. Colloid Interface Sci.* **361** 278
80. Page K and Monson P 1996 *Phys. Rev. E* **54** 6557
81. Malani A, Ayappa K G and Murad S 2009 *J. Phys. Chem. B* **113** 13825
82. Kamakshi J and Ayappa K G 2001 *Langmuir* **17** 5245
83. Ayappa K G and Ghatak C 2002 *J. Chem. Phys.* **117** 5373
84. Malani A and Ayappa K G 2012 *Mol. Simul.* **38** 1114
85. Saharay M and Balasubramanian S 2007 *J. Phys. Chem. B* **111** 387
86. Plimpton S 1995 *J. Comput. Phys.* **117** 1
87. Harris J G and Yung K H 1995 *J. Phys. Chem.* **99** 12021
88. Fujita M, Oguro D, Miyazawa M, Oka H, Yamaguchi K and Ken-taro Ogura 1995 *Nature* **378** 469
89. Mera H A, Gomez-Ballesteros J L and Balbuena P B 2014 *J. Chem. Eng. Data* **59** 2973
90. Eslami H, Kesik M, Karimi-Varzaneh H A and Müller-Plathe F 2013 *J. Chem. Phys.* **139** 124902
91. Bhatia S K and Myers A L 2006 *Langmuir* **22** 1688
92. Plant D F, Maurin G and Bell R G 2007 *J. Phys. Chem. B* **111** 2836
93. Rosi N L, Eckert J, Eddaoudi M, Vodak D T, Kim J, O'Keeffe M and Yaghi O M 2003 *Science* **300** 1127
94. Queen W L, Hudson M R, Bloch E D, Mason J A, Gonzalez M I, Lee J S, Gygi D, Howe J D, Lee K, Darwish T A, James M, Peterson V K, Teat S J, Smit B, Neaton J B, Long J R and Brown C M 2014 *Chem. Sci.* **5** 4569
95. Ogilvie S H, Duyker S G, Southon P D, Peterson V K and Kepert C J 2013 *Chem. Commun.* **49** 9404
96. MCIN is available for academic users on request by email to the Corresponding Author